

## Influence of the Impact Limiter Shape on the Impact Absorbing Behavior According to the Cask Type

150

가

A B

가

가

### Abstract

All radioactive material transportation packages are required to maintain their structural safety under the hypothetical accident conditions such as free drop impact prescribed as a regulation in atomic law. Impact limiters which attached at the outer ends of the packages use a foam-filled steel shell structures, in which the buckling of thin walled structure and the crush deformation behavior are used together for energy absorbing mechanism. For the thin walled structures, in spite of the same dimensions and thicknesses, the buckling behaviors are changed quite differently according to the boundary conditions. The packages are classified into A or B-type according to the contents of the radioactive material. In this study, the variation of impact absorbing behaviors according to the change of corner shape variation of impact limiters for the same package if it is classified differently, and some comments for effective impact limiter design are suggested.

1.

[1] 가

, 가

[2].

[3].

Fig. 1

-

, 60%

가

(lock-up)

가

. Fig. 2

가

-

.

가

가

가

,

(densification region)

가

. Fig. 3

가

(crush)

,

[4].

(buckling coefficient)가

(a/b)

가

,

가

가 ,

가

가 2 mm

9m

A B

가 1.2m B

가

가

## 2.

### 2.1

430 mm, 320 mm, 380 kg

가

(curvature)

가

Fig. 5

LS-DYNA [5]

Fig. 4

1/2

1/4

3

가 1/2

19,680

13,920

2,688

가

(single surface contact)

(buckling)

가

가

가

가

가

1.2m

9 m

4.85 m/s

13.3 m/s

가

(impact target surface)

2.2

. Fig. 6

. Fig. 7 A  
. Fig. 7(a)

A B  
가 가

가

가

B

Fig. 7(b)

. A B  
Table 1 2

2.2

가

. Fig. 8

. Fig. 9 A  
. Fig. 9(a)

A B  
가 가

가

가

. B

Fig. 7(b)

가

가 가

가

가

가

. A B  
Table 1 2

3.

가

가

가

Table 1 Fig. 7(a)

A

가  
6.4 ms

가

42%

Table 2 Fig. 7(b)

B

가

가

18%

가

50%

가

가

Table 1 Fig. 7(a)

A

가

가

가

가

가

가

가

가

가

B

가

가

가 A

1.2m

가 4.85 m/s

B

가 9m

가 13.3 m/s

A

가

가

B

가

가

B

가

가

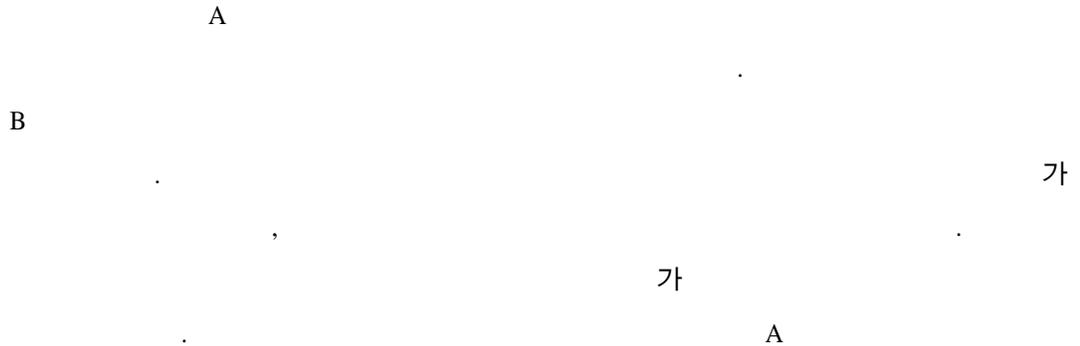
Table 1. Max. Impact Forces of A-Type Package

Drop Orientation	Impact Limiter Shape	Max. Impact Force (kN)	Time at Max. Impact Force Occurs (ms)	Impact Duration(ms)
Vertical	Rectangular	599.9	0.2	6.4
	Round corner	251.5	2.8	9.6
	Circular	212.7	8.0	12.0
Horizontal	Rectangular	258.3	7.4	19.8
	Round corner	271.4	7.8	20.2
	Circular	291.3	10.6	20.2

Table 2. Max. Impact Forces and Displacements of B-Type Package

Drop Orientation	Impact Limiter Shape	Max. Impact Force (kN)	Max. Disp.(mm)	Max. g-value
Vertical	Rectangular	2,029(2.9)	22.9(3.0)	554(2.5)
	Round corner	2,113(3.1)	23.7(3.0)	578(3.0)
	Torus	2,146(2.8)	23.8(3.0)	582(2.6)
Horizontal	Rectangular	1,257(4.6)	39.8(5.0)	343(4.5)
	Round corner	1,518(4.6)	40.2(5.0)	413(4.5)
	Torus	1,458(5.2)	45.7(5.5)	389(4.6)

4.



- [1] IAEA Safety Standards Series No. ST-1, "Regulations for the Safe Transport of Radioactive Material," IAEA, 1996.
- [2] Lampinen, B. E. and Jeryan, R. A., "Effectiveness of Polyurethane Foam in Energy Absorbing Structures," *Trans. SAE 91*, pp. 2059-2076 (1982).
- [3] Wellman, G. W., Transportation System Impact Limiter Design using Rigid Polyurethane Foam, SAND84-2271 DE85 015088, Sandia National Laboratories, 1984.
- [4] Johnston, J. E., "Guide to Stability Design Criteria for Metal Structures," Structural Stability Research Council, John Wiley and Sons Inc., 3rd. ed., 1976.
- [5] Hallquist, J. O., 1991, "LS-DYNA3D Theoretical Manual," LSTC Report 1018, Livermore Software Technology Corporation, USA.

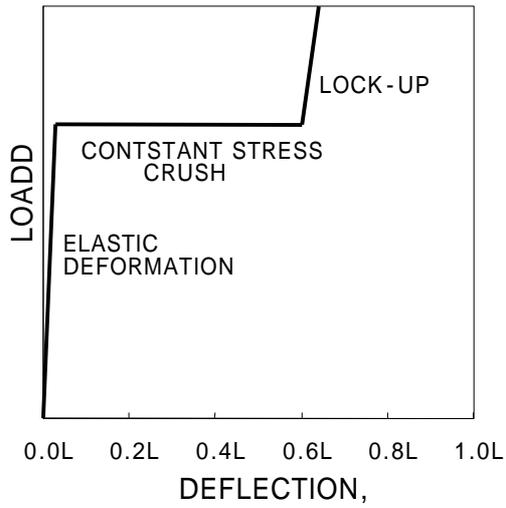


Fig. 1 Idealized crush load-deflection curve of the impact limiter.

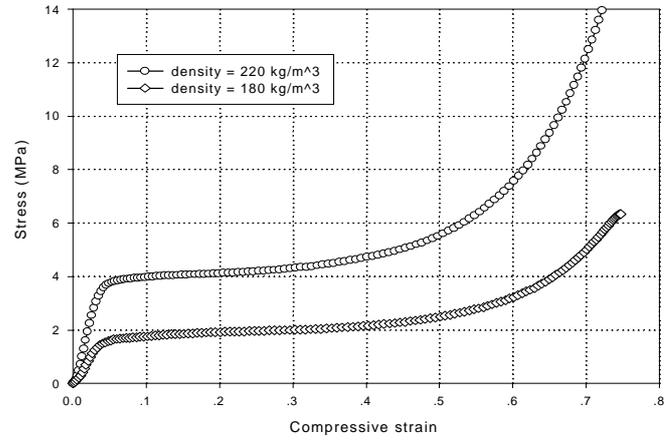
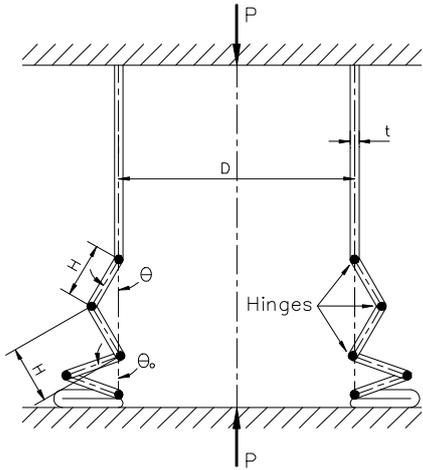
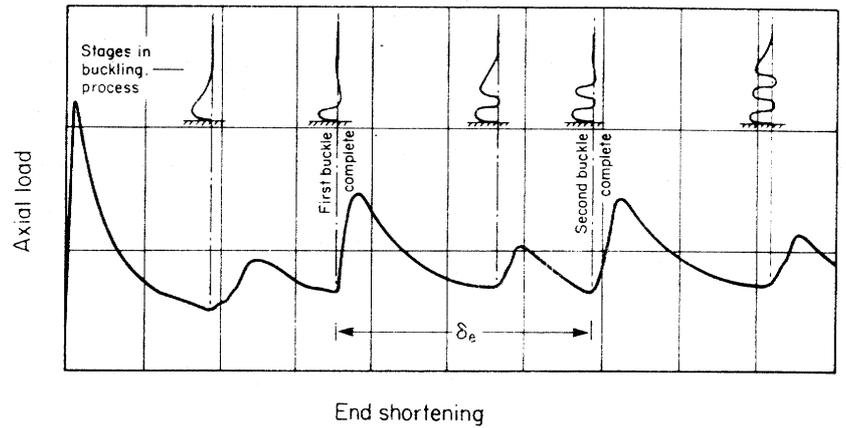


Fig. 2 Load-deflection curves of polyurethane foams.



(a) idealized deformation for concertina mode of buckling



(b) relationship between deformed shape and shape of load-deflection curve

Fig. 3. An idealized model of axisymmetric concertina buckling of axially compressed cylindrical tube.

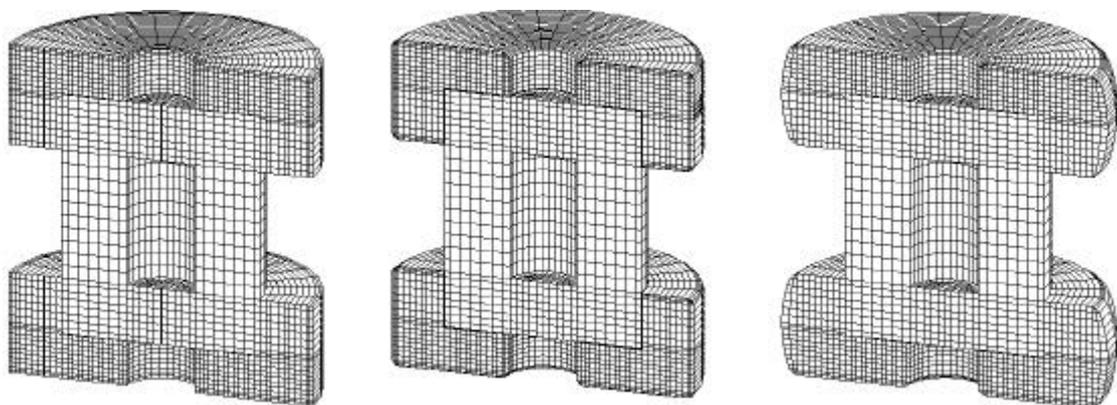


Fig. 4. Impact analysis models of cask for vertical drop for each impact limiter shape.

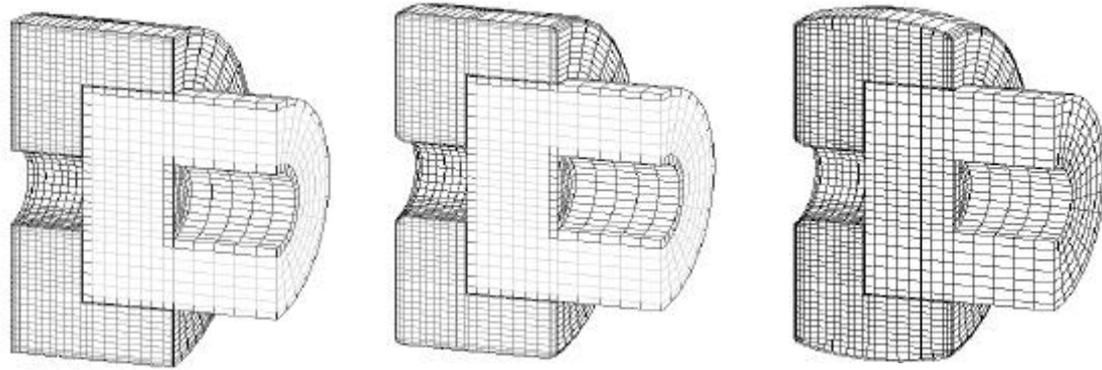


Fig. 5. Impact analysis models of cask for horizontal drop for each impact limiter shape.

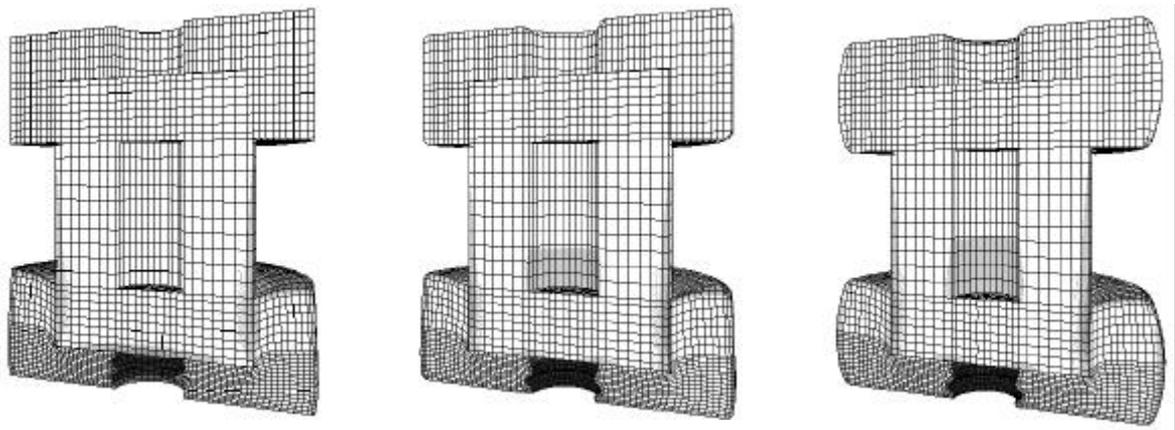
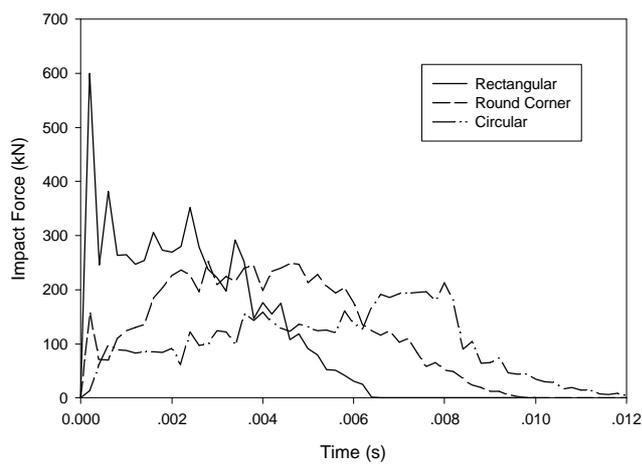
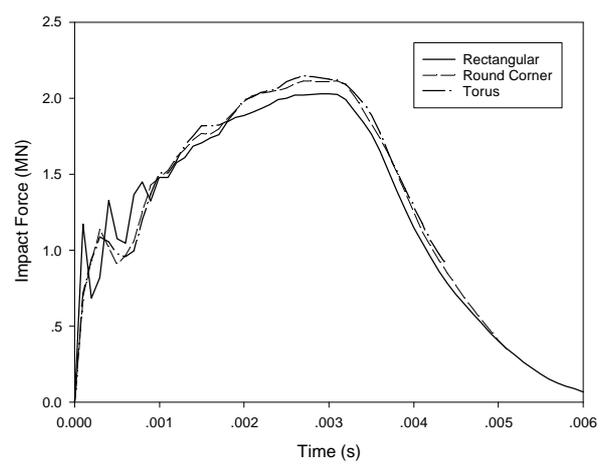


Fig. 6. Stress contours and deformed shapes of cask for vertical drop for each impact limiter shape.



(a) A-type cask



(b) B-type cask

Fig. 7. Comparison of impact force-time histories of under vertical drop for impact limiter shape variation.

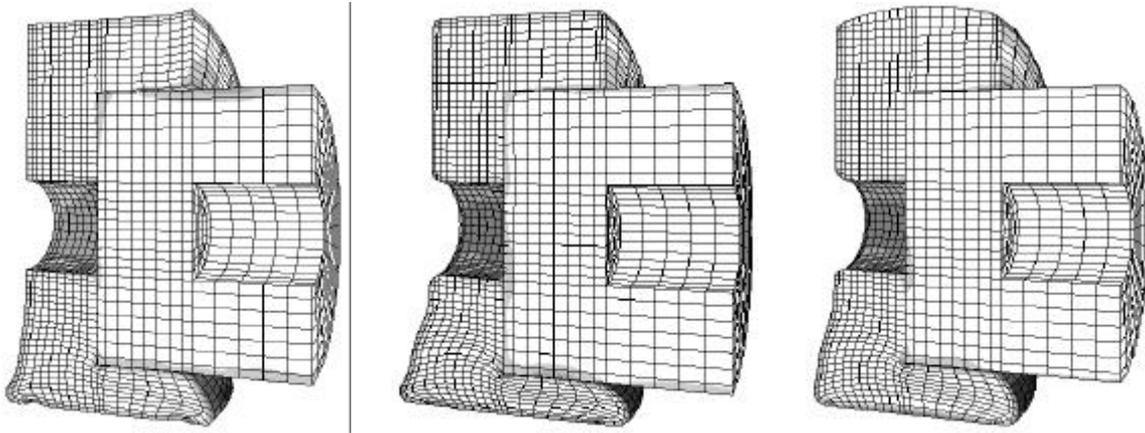
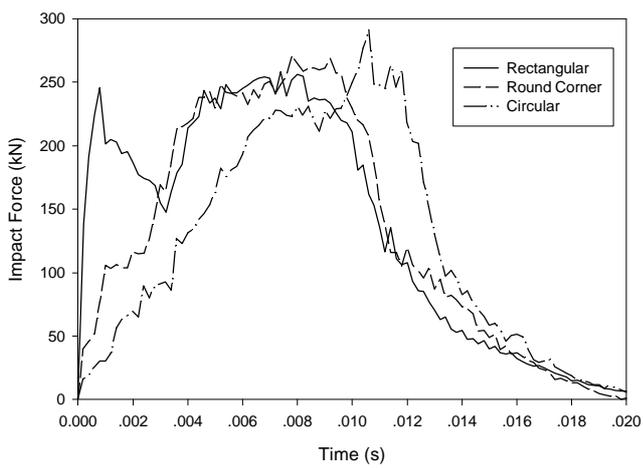
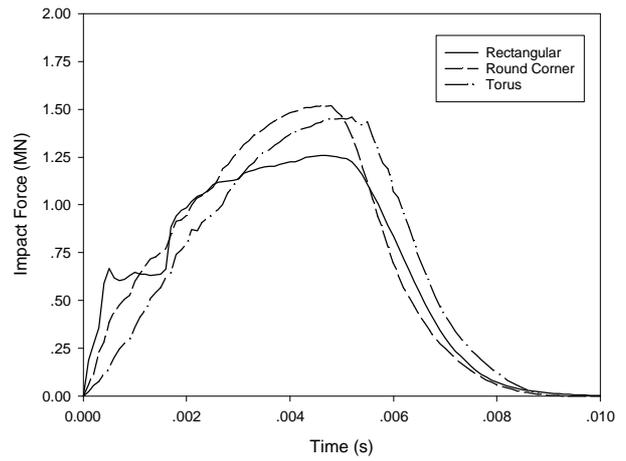


Fig. 8. Stress contours and deformed shapes of cask under horizontal drop for each impact limiter shape.

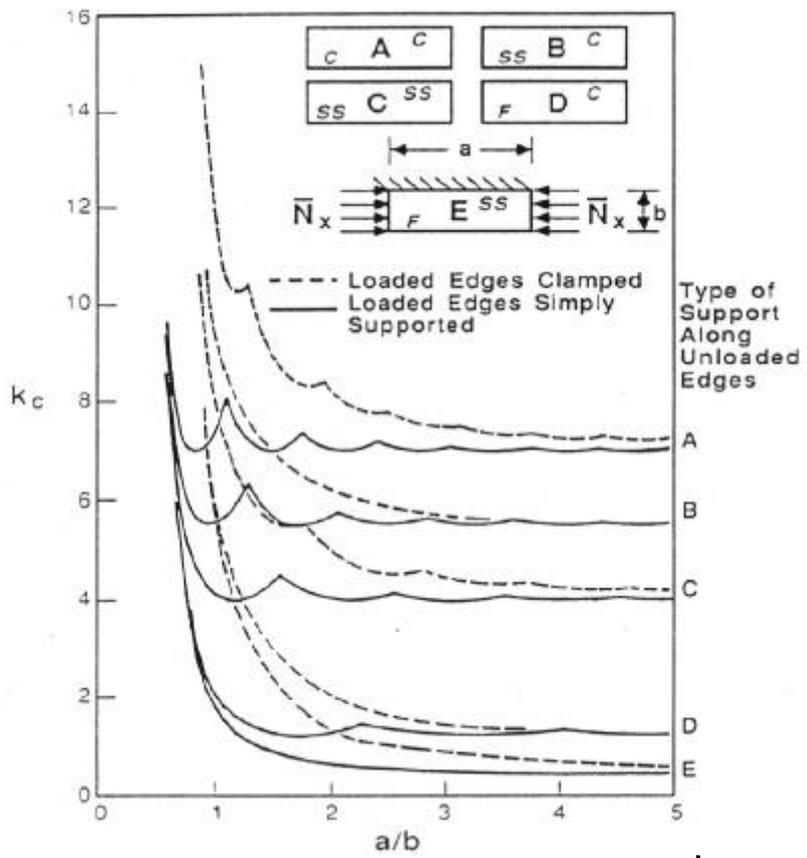


(a) A-type cask



(b) B-type cask

Fig. 9 Comparison of impact force-time histories of under vertical drop for impact limiter shape variation.



Compressive-buckling coefficients for flat rectangular plates

